Towards many-dimensional real-time quantum theory for heavy-particle dynamics. I. Semiclassics in the Lagrange picture of classical phase flow

Satoshi Takahashi and Kazuo Takatsuka
Department of Basic Sciences, Graduate School of Arts and Sciences, The University of Tokyo, Komaba 153-8902, Tokyo, Japan
(Received 9 June 2013; published 14 January 2014)

We study a quantum theory in terms of action decomposed function (ADF), a class of quantum wave function, towards many-dimensional applications to quantum dynamics of heavy particles as in chemical reactions. The equation of motion for the complex-valued amplitude of ADF represents a coupling between the internal diffusive motion of a wave packet and dynamics of its group velocity in a hierarchical manner ascending from classical to purely quantum mechanics via semiclassical dynamics. We attempt to solve this equation of motion dividing it into two stages: a semiclassical level and beyond. In this paper, as the first stage, we develop a semiclassical approximation in the Lagrange picture of classical phase flow. In the Euler picture (as in the standard WKB picture), continuous integration of the stability matrix along the paths is required. By adopting the Lagrange picture, on the other hand, we represent the semiclassical amplitude in terms of what we call deviation determinant, which can be evaluated readily in many-dimensional systems. Numerical tests show that ADF reproduces quantum wave packets at each space-time point along classical paths very well. However, the ADF in this stage is not free of the semiclassical singularity. In other words, the wave functions diverge at turning points or caustics, depending on the initial conditions chosen. This divergence is known to take place at points where classical paths smoothly distributed in phase space have "focuses" in configuration space (or momentum space) and reflects an intrinsic relationship between quantum and classical mechanics. Therefore, it is by studying the mechanism of removing the singularity that the essential feature of quantum mechanics will be clarified. This aspect will be discussed in a companion paper [K. Takatsuka and S. Takahashi, Phys. Rev. A **89**, 012109 (2014)] as the second stage of many-body quantum theory.

DOI: 10.1103/PhysRevA.89.012108 PACS number(s): 03.65.Ca, 03.65.Sq, 34.10.+x, 31.15.−p

I. INTRODUCTION

Asymptotic analysis has revealed that there lies a deep discrepancy in-between quantum and classical mechanics reflecting a difference in their mathematical structures [1]. In particular, the stationary phase approximation (SPA) applied in reducing the Feynman path integrals to its semiclassical representation [2,3], under an assumption of small $\hbar$ as in dynamics of nuclei in molecules, frequently brings about divergence in the amplitude of a semiclassical wave function and related quantities [2,3]. This divergence is intuitively attributed to a singular projection of phase-space distribution of classical trajectories onto configuration space in representing a quantum wave function. More precisely, the SPA applied to the Feynman kernel gives, for instance,

$$K(\mathbf{q}_f,\mathbf{q}_i,t) \equiv \langle \mathbf{q}_f | \exp\left[-\frac{i}{\hbar}\hat{H}t\right]|\mathbf{q}_i\rangle \simeq (2\pi\hbar)^{-N/2}\left|\frac{\partial \mathbf{q}_f}{\partial \mathbf{p}_i}\right|^{-\frac{1}{2}} \exp\left[\frac{i}{\hbar}S(\mathbf{q}_f,\mathbf{q}_i,t) - \frac{i\pi\lambda}{2}\right], \tag{1}$$

where $\mathbf{q}_f$ and $\mathbf{q}_i$ are the end points of an N-dimensional classical path generated by a Hamiltonian H for a time t, S is the classical action integral along the path, and $\partial\mathbf{q}_f/\partial\mathbf{p}_i$ is a minor determinant of the so-called stability matrix $[\partial(\mathbf{q}_f,\mathbf{p}_f)/\partial(\mathbf{q}_i,\mathbf{p}_i)]$. The preexponential factor $|\partial\mathbf{q}_f/\partial\mathbf{p}_i|^{-1/2}$ diverges at every caustic point due to zeros of $\partial\mathbf{q}_f/\partial\mathbf{p}_i$, whereby the Maslov phase is to be accumulated as much as $-\pi\lambda/2$ at each passage across zero with λ being the number of passages. Aside from the singularity, the computation of the stability matrix along an N-dimensional classical path needs continuous integration of coupled ordinary differential equations of $2N \times 2N$ dimensions. Furthermore, to carry out this integration, one has to calculate an $N \times N$ Hessian matrix (the second-order derivatives) of the potential function involved, which is not easy to do for complicated potential functions in high dimensions.

To overcome these difficulties, many works have been devoted in the long history. A classic approach to deal with the singularities is the so-called uniform approximation. In the case where two or more roots coalesce in the stationary phase conditions applied to oscillatory integrals such as those involving path summations, one has to include the terms higher than the second order into the phases [4–8]. This way of unfolding the singularity is mathematically interesting, but incorporating higher-order terms one by one is generally not suitable for many-dimensional applications. We also recall the higher-order WKB approximations, the Maslov recursive transport equations of quantum dynamics [1], and a perturbation theoretic $\hbar$ expansion of the Wigner phase-space distribution function [9,10]. However, applications of these recursive and perturbative methods to systems of higher than two dimensions have not been performed yet.

On the other hand, those singularities as in Eq. (1) have been removed by various semiclassical methods in such ways as coordinate transformation [in the so-called initial value representation (IVR) [11–13]], assuming a potential function to be quadratic everywhere [14], lifting semiclassical mechanics into phase space [15,16]. Among others, the IVR and the so-called Herman-Kluk (sometimes referred to as Heller-Herman-Kluk-Kay) representations [17–21] are now recognized as practical methods for chemical reaction dynamics. Furthermore, there have been proposed

practical approximations to reduce the computational efforts in multidimensions, including separable approximation for the prefactor and time averaging in semiclassical molecular spectra [22–24], prefactor-free semiclassical propagation by averaging in phase space and in time [25], prefactor-free semiclassical on-the-fly computation [26], and linearization approximation to the double phase-space integral expression of the semiclassical time correlation function, leading to only a single phase-space expression [27–30] [for an application of this approximation to devise a practical propagation method based on the Herman-Kluk propagator (see [31])] along with an efficient method to accelerate the numerical computations related to the potential Hessians [32]. Moreover, the Herman-Kluk propagator has been shown to arise as the lowest-order term of a series expansion to represent the exact quantum propagator, either in a perturbative expansion [33–37] or in an $\hbar$-series expansion [38–42].

With the advent of current massive parallel computers, it has become increasingly more feasible to perform the larger-scale molecular dynamics simulations. In the studies of real-time chemical dynamics, it is desirable that quantum dynamics is appropriately described along classically propagated trajectories. Despite the theoretical developments as above, quantum many-body real-time dynamics is still worth further study in various aspects. Besides, precise analysis of the quantum-classical correspondence may be linked to interpretation and understanding in depth of the essential features of quantum mechanics that differentiates it from classical mechanics. In this and companion papers, we study an approximate quantum theory for many-dimensional real-time quantum dynamics, by tracking a different route from those referred to as above. Our proposed dynamics incorporates the quantum effects without resorting to the $\hbar$ series. It is based on a propagation of a bundle of classical trajectories rather than the stability matrix calculation, and hence no computation of the potential Hessian matrix is demanded [43]. This is crucial in practice not only for large-dimensional systems having complicated potential energy functions, but also even in lower-dimensional *ab initio* quantum-chemistry calculations with use of highly correlated electronic wave functions. *Ab initio* molecular dynamics, or the first-principles calculations with classical trajectories on accurate potential energy surfaces (PES), is now readily applied to chemical dynamics, thanks to the progress in very accurate quantum-chemical methodology that successfully provides the analytical expressions of the energy gradient [44]. On the other hand, it is sometimes the case that the analytical expressions of the second derivative for highly accurate *ab initio* PESs are not yet formulated.

This work is described in two papers: paper I, this paper, is devoted to development in the first stage up to the many-dimensional semiclassics, and paper II, a following companion paper, proposes a theory to cope with the second stage beyond semiclassical singularity [45]. In both papers, we study a quantum wave-packet dynamics in terms of what we call action decomposed function (ADF). After reviewing the structure of the equation of motion for ADF, we propose in this paper a theory in the level of semiclassical approximation but without using the stability matrix. Being free of the factor such as $|\partial \mathbf{q}_f/\partial \mathbf{p}_i|^{-\frac{1}{2}}$ in Eq. (1), the method can be applied to many-dimensional systems as exemplified later. However, this semiclassical ADF is not free of divergence at caustics or turning points.

In paper II, we proceed to the realm where the singularities are naturally removed in a tractable manner. The critical notion behind this procedure is quantum smoothing due to "quantum diffusion" having an imaginary diffusion constant (implicitly suggesting a stochastic dynamics behind), which brings an $\hbar$ dependence into the amplitude of ADF and thereby smooths the singularity. Since the theory is built in a stepwise manner, we proceed to the goal verifying the underlying ideas with numerical examinations in each step.

This paper is organized as follows: We first summarize in Sec. II the equation of motion for the amplitude factor of ADF. Section III reviews the ADF in the standard WKB-like picture, which is based on the Euler picture of classical phase flow. We then show in Sec. IV how the semiclassical ADF can be represented in terms of the so-called deviation determinant. The validity and accuracy of the basic idea are examined in Sec. V, which also exposes the limitation of the semiclassical approximation. We demonstrate that large-scale systems are indeed treated in a tractable manner. The paper concludes in Sec. VI with some remarks.

II. ACTION DECOMPOSED FUNCTION

A. Definition and equation of motion

Let us begin with the following time- (t-) dependent wave function:

$$\Psi(\mathbf{q},t) = F(\mathbf{q},t)\exp\left(\frac{i}{\hbar}S(\mathbf{q},t)\right) \tag{2}$$

on a point $\mathbf{q}$ in configuration space, where $S(\mathbf{q},t)$ is assumed to satisfy the Hamilton-Jacobi (HJ) equation

$$\frac{\partial S(\mathbf{q},t)}{\partial t} + \frac{1}{2m}[\nabla S(\mathbf{q},t)]^2 + V(\mathbf{q}) = 0, \tag{3}$$

where m collectively represents the masses of particles [46]. In Eq. (2), $\exp[\frac{i}{\hbar}S(\mathbf{q},t)]$ is regarded as a transformation function to determine the unknown function $F(\mathbf{q},t)$. The equation of motion for this is then given as

$$\frac{\partial F(\mathbf{q},t)}{\partial t} = \left(-\mathbf{p}\cdot\nabla - \frac{1}{2}(\nabla\cdot\mathbf{p})\right)F(\mathbf{q},t) + \frac{i\hbar}{2}\nabla^2 F(\mathbf{q},t), \tag{4}$$

where $\mathbf{p}$ is a momentum at $(\mathbf{q},t)$ as

$$\mathbf{p} = \nabla S(\mathbf{q},t). \tag{5}$$

We use throughout the paper the mass-weighted coordinates that scale all the masses to unity ($m = 1$), and hence numerically $\mathbf{p} = \mathbf{v}$.

Since dynamics arising from the group velocity of $\Psi(\mathbf{q},t)$ is taken into account by the HJ equation, Eq. (4) is responsible for representing only the kinematics of the shape-changing motion inside the wave packet. The first two terms of the right-hand side of Eq. (4) represent the coupling between the kinematics and the group motion, and the last one reflects the (quantum) diffusive motion having a diffusion constant of pure imaginary value. It is noticed that the "diffusion operator" in Eq. (4) is of the same form as that of the total kinetic energy operator in the original Schrödinger equation. However, $\frac{i\hbar}{2}\nabla^2$ in Eq. (4) is responsible only for kinematics within the wave packet since

kinetic energy due to the group velocity of external motion of the packet has already been separated out by the HJ equation. In other words, the Schrödinger equation collectively treats the two roles of kinematics in a single Laplacian.

By the way, since we plan to apply the ADF to chemical dynamics under laser fields, we need to know how the above equation of motion Eq. (4) should be modified. As shown in the Appendix, it turns out that the equation of motion is of the exactly same form in classical electromagnetic vector fields. This is because the ADF equation arises only from the kinematic part of the Schrödinger equation. Some preliminary applications are seen in Ref. [47]. Once one specifies a point $(\mathbf{q},t)$ on an action surface $S(\mathbf{q},t)$, $\mathbf{p}(\mathbf{q},t)$ is also automatically specified on a classical path due to Eq. (5). Thus, $F(\mathbf{q},t)$ is determined on a classical trajectory.

B. From Euler picture to Lagrange one: Simplification of the dynamics

Rewriting Eq. (4) as

$$\left(\frac{\partial}{\partial t}+\mathbf{p}\cdot\boldsymbol{\nabla}\right)F(\mathbf{q},t)=-\frac{1}{2}(\boldsymbol{\nabla}\cdot\mathbf{p})F(\mathbf{q},t)+\frac{i\hbar}{2}\nabla^2F(\mathbf{q},t), \tag{6}$$

we have a time-derivative operator moving along a flow line defined in the vector field of $\mathbf{p}(\mathbf{q},t)$:

$$\frac{D}{Dt}=\frac{\partial}{\partial t}+\mathbf{p}\cdot\boldsymbol{\nabla}, \tag{7}$$

and the equation of motion is reformulated as

$$\frac{D}{Dt}F(\mathbf{q},t)=\left[-\frac{1}{2}(\boldsymbol{\nabla}\cdot\mathbf{p})+\frac{i\hbar}{2}\nabla^2\right]F(\mathbf{q},t). \tag{8}$$

In analogy to fluid dynamics, we refer to the presentation of Eq. (4) as the Euler picture, while Eq. (8) as the Lagrange picture. The seeming difference between the two is only $-\mathbf{p}\cdot\boldsymbol{\nabla}F(\mathbf{q},t)$, but its consequence is not small. In what follows, we write $F(\mathbf{q},t)$ as $F(\mathbf{q}-\mathbf{q}(t),t)$ to note that the dynamics is described along the classical flow lines $\mathbf{q}(t)$.

In practical calculations, the Trotter decomposition

$$F(\mathbf{q}-\mathbf{q}(t+\Delta t),t+\Delta t)\simeq\exp\left[-\frac{1}{2}(\boldsymbol{\nabla}\cdot\mathbf{p})\Delta t\right]\exp\left[\frac{i\hbar}{2}\Delta t\nabla^2\right]F(\mathbf{q}-\mathbf{q}(t),t) \tag{9}$$

or

$$F(\mathbf{q}-\mathbf{q}(t+\Delta t),t+\Delta t)\simeq\exp\left[\frac{i\hbar}{2}\Delta t\nabla^2\right]\exp\left[-\frac{1}{2}(\boldsymbol{\nabla}\cdot\mathbf{p})\Delta t\right]F(\mathbf{q}-\mathbf{q}(t),t) \tag{10}$$

can be applied. To reduce possible error in this approximation, Δt should be taken appropriately small. The operator ordering is somewhat a tedious problem, but our final results do not depend on it.

C. Hierarchical structure from classical mechanics to quantum theory

In the dynamics of Eq. (8), we observe a very simple hierarchical structure from classical to full quantum mechanics as follows.

Classical flow. First, nullify as the most crude approximation all the terms in the right-hand side of Eq. (8) as

$$\left.\frac{DF(\mathbf{q}-\mathbf{q}(t),t)}{Dt}\right|_{\mathbf{q}=\mathbf{q}(t)}=0. \tag{11}$$

Since the time derivative D/Dt is explicitly defined on a classical trajectory [one of solutions of Eq. (3)] in Eq. (7), the solution of Eq. (11) is obtained in a straightforward way as

$$|F(\mathbf{q}-\mathbf{q}(t),t)|_{\mathbf{q}=\mathbf{q}(t)}|^2=|F(\mathbf{q}-\mathbf{q}(0),0)|_{\mathbf{q}=\mathbf{q}(0)}|^2. \tag{12}$$

Thus, the absolute height of the classical ADF is preserved along a relevant path $[\mathbf{q}(t),\mathbf{p}(t)]$, and the shape change of the total wave packet is represented by geometrical redistribution of classical trajectories. The conservation of probability is secured by Eq. (12) and the classical Liouville theorem.

Semiclassical flow. By including the term of "divergence" $(\boldsymbol{\nabla}\cdot\mathbf{p})$ to the classical approximation as

$$\frac{DF(\mathbf{q}-\mathbf{q}(t),t)}{Dt}=-\frac{1}{2}(\boldsymbol{\nabla}\cdot\mathbf{p})F(\mathbf{q}-\mathbf{q}(t),t), \tag{13}$$

we can consider the dynamical change of the nearby region of a reference path $[\mathbf{q}(t),\mathbf{p}(t)]$. In what follows, we call $\boldsymbol{\nabla}\cdot\mathbf{p}$ "momentum gradient" to avoid confusion by using the word "divergence." It can be readily proven that the quantum probability is reserved in this dynamics, as will be seen later. This level of approximation is essentially equivalent to the lowest-order WKB approximation [46].

Full quantal flow. We then retrieve the complete form of right-hand side by further adding the term of quantum diffusion

$$\frac{DF(\mathbf{q}-\mathbf{q}(t),t)}{Dt}=\left[-\frac{1}{2}(\boldsymbol{\nabla}\cdot\mathbf{p})+\frac{i\hbar}{2}\nabla^2\right]F(\mathbf{q}-\mathbf{q}(t),t). \tag{14}$$

Note that only in this level, the Planck constant emerges in the amplitude function $F(\mathbf{q}-\mathbf{q}(t),t)$. In this series of works, we attempt to solve approximately this equation without resorting to perturbation expansion in $\hbar$ and to the stationary phase approximation.

The above hierarchical structure in-between classical and quantum mechanics is also useful in the application of hybrid use of quantum-semiclassical-classical representation of dynamics. For instance, in a protein dynamics, the skeletal structure may be well treated in classical simulation, while other interacting parts may need quantum and/or semiclassical descriptions.

D. Linearity

We here compare the ADF with the Bohm trajectory method since they are seemingly look-alike. (For the great progress in the relevant methodology achieved by Wyatt and his co-workers, see [48–51]. About the applications of quantum trajectories, see also [52–56]. Furthermore, refer to [57–61] for a generalization of the Bohmian dynamics or quantum trajectory method.) Let us first summarize the Bohm theory briefly [62]. Represent a wave function as

$$\Psi(\mathbf{q},t)=R(\mathbf{q},t)\exp\left(\frac{i}{\hbar}S(\mathbf{q},t)\right), \tag{15}$$

where both R and S are real-valued functions. The equations of motion for them are

$$\frac{\partial R}{\partial t} + \nabla S \cdot \nabla R + \frac{R}{2}\nabla^2 S = 0 \tag{16}$$

and

$$\frac{\partial S}{\partial t} + \frac{1}{2m}(\nabla S)^2 + V - \frac{\hbar^2}{2m}\frac{\nabla^2 R}{R} = 0. \tag{17}$$

The first equation is nothing but the equation of continuity, that is,

$$m\frac{\partial \rho}{\partial t} + \nabla \cdot (\mathbf{v}\rho) = 0, \tag{18}$$

where

$$\rho = R^2 \tag{19}$$

and

$$\mathbf{v} = \nabla S. \tag{20}$$

Usually, the Bohm method is not regarded as a semiclassical theory, simply because R is not expanded in a power of the Planck constant as in the WKB theory.

As is widely recognized everything interesting and drawbacks as well are found in the quantum potential $-\frac{\hbar^2}{2m}\frac{\nabla^2 R}{R}$, in which the quantum effects are all concentrated. On the other hand, this potential can be singular at points $R = 0$ and nonlocal. Moreover, the "quantum path solutions" are driven by the potential that is to be constructed with the solution of the Schrödinger equation itself. In this sense, the equation is essentially nonlinear. This is in marked contrast to the ADF equation of motion

In this conjunction, it is instructive to note that stochastic quantization by Nelson is also nonlinear [63]. He establishes a forward and backward stochastic Newtonian-type equation that contains a drift term. This is transformed to a Fokker-Planck equation, which is further rewritten to the Schrödinger equation in the end. However, the drift term involved in the stochastic equation can be evaluated only in terms of the knowledge of the distribution function (corresponding to the wave function), and the stochastic path should be determined consistently with this distribution. On the other hand, the distribution function in turn is to be determined by the ensemble of the paths. Therefore, the stochastic paths and their distribution are to be determined only in a nonlinear manner. By contrast, ADF dynamics is of a linear type in that it does not require the knowledge of distribution beforehand. The ADF implicitly contains a stochastic process driven by the imaginary diffusion constant, which will be studied in paper II [45].

III. TRADITIONAL SEMICLASSICAL THEORY IN EULER PICTURE WITH USE OF THE STABILITY MATRIX

A. WKB-like solution

The semiclassical equation of motion for the function $F(\mathbf{q},t)$ looks as

$$\frac{\partial F}{\partial t} + \mathbf{p} \cdot \nabla F = -\frac{1}{2}(\nabla \cdot \mathbf{p})F, \tag{21}$$

where $\mathbf{p}(t) = \partial S_2(\mathbf{q},\mathbf{p}_0,t)/\partial \mathbf{q}$ is the classical momentum. We here use S_2 as an action function, which starts from a momentum and ends with a configuration space. Equation (21) is integrated as follows. We start from the following observation:

$$\frac{\partial F^2}{\partial t} + \nabla \cdot (\mathbf{p}F^2) = 0. \tag{22}$$

Note that F^2 rather than $|F|^2$ is considered in this "equation of continuity" (notice that F^2 can be complex). F^2 can be readily integrated locally along classical paths in terms of a Jacobian determinant $\partial \mathbf{q}_t/\partial \mathbf{q}_0$ which is also a minor determinant of the so-called stability matrix. It is not difficult to derive the equation

$$\frac{\partial}{\partial t}\left(\frac{\partial \mathbf{q}_t}{\partial \mathbf{q}_0}\right)^{-1} + \nabla \cdot \left[\mathbf{p}\left(\frac{\partial \mathbf{q}_t}{\partial \mathbf{q}_0}\right)^{-1}\right] = 0 \tag{23}$$

from the Hamilton-Jacobi equation for $S_2(\mathbf{q}_t,\mathbf{p}_0,t)$. Furthermore, one has the initial condition $(\partial \mathbf{q}_t/\partial \mathbf{q}_0)^{-1} = 1$ since $\mathbf{q}_t = \mathbf{q}_0$ at $t = 0$. Thus, $(\partial \mathbf{q}_t/\partial \mathbf{q}_0)^{-1}$ can be regarded as a local representation of the Green's function for the propagator of Eq. (22). On comparing Eqs. (22) and (23), together with the initial conditions above, one immediately has [46,64]

$$\begin{aligned} F(\mathbf{q}_t,t) &= F(\mathbf{q}_0,0)\left(\frac{\partial \mathbf{q}_t}{\partial \mathbf{q}_0}\right)^{-\frac{1}{2}} \\ &= F(\mathbf{q}_0,0)\left|\frac{\partial \mathbf{q}_t}{\partial \mathbf{q}_0}\right|^{-\frac{1}{2}} \exp\left[-\frac{i\pi M(\mathbf{q}_0,\mathbf{q}_t)}{2}\right], \end{aligned} \tag{24}$$

where the derivative $\partial \mathbf{q}_t/\partial \mathbf{q}_0$ is taken under the fixed initial momentum $\mathbf{p}_0$, and $M(\mathbf{q}_0,\mathbf{q}_t)$ is the Maslov index in this representation that counts the number of zeros of $\partial \mathbf{q}_t/\partial \mathbf{q}_0$ up to the degeneracy. Thus, the local solution, denoted by $\Psi^{\mathbf{p}_0}_{\text{local}}(\mathbf{q}_t,t)$, is evolved in time on an action surface, which is in turn to be propagated in terms of trajectories of a fixed initial momentum $\mathbf{p}_0$. The final expression for the wave function is then written in the form of IVR as

$$\begin{aligned} \Psi_{p_0}(\mathbf{q},t) &= \int \delta(\mathbf{q}-\mathbf{q}_t)\Psi^{\mathbf{p}_0}_{\text{local}}(\mathbf{q}_t,t)d\mathbf{q}_t \\ &= \int \delta[\mathbf{q}-\mathbf{q}_t(\mathbf{q}_0,\mathbf{p}_0)]F(\mathbf{q}_0,0)\left|\frac{\partial \mathbf{q}_t}{\partial \mathbf{p}_0}\right|^{\frac{1}{2}} \\ &\quad \times \exp\left[\frac{i}{\hbar}S_2(\mathbf{q}_t,\mathbf{p}_0,t) - \frac{i\pi M(\mathbf{q}_0,\mathbf{q}_t)}{2}\right]d\mathbf{q}_0, \end{aligned} \tag{25}$$

and therefore no divergence in the integrand.

Upon comparing this expression with the IVR of the WKB-like semiclassical kernel, which is

$$\begin{aligned} \Psi(\mathbf{q},t) &= (2\pi\hbar)^{-N/2}\int \delta[\mathbf{q}-\mathbf{q}_t(\mathbf{q}_0,\mathbf{p}_0)]\Psi(\mathbf{q}_0,0)\left|\frac{\partial \mathbf{q}_t}{\partial \mathbf{p}_0}\right|^{\frac{1}{2}} \\ &\quad \times \exp\left[\frac{i}{\hbar}S(\mathbf{q}_t,\mathbf{q}_0,t) - \frac{i\pi\lambda(\mathbf{q}_0,\mathbf{q}_t)}{2}\right]d\mathbf{q}_0 d\mathbf{p}_0, \end{aligned} \tag{26}$$

we immediately realize that the semiclassical ADF is decomposed into each sheet of the momentum space specified by the initial momentum $\mathbf{p}_0$. This property may be used to reduce the dimension of phase-space integration dramatically as suggested by the difference between $d\mathbf{q}_0$ in Eq. (25) and $d\mathbf{q}_0 d\mathbf{p}_0$ in Eq. (26) [64–73].

B. Conservation relation in half-density-like representation

The above results can be represented in a more compact form. Define "square root" of the volume element in semiclassical integrals for an arbitrary function $f(\mathbf{q}_t,t)$, which is to be carried by the classical flow in such a way that

$$I = \int f(\mathbf{q}_t,t)d\mathbf{q}_t = \int f(\mathbf{q}_t,t)d\mathbf{q}_t^{1/2}d\mathbf{q}_t^{1/2*} \tag{27}$$

and

$$d\mathbf{q}_t^{1/2} \equiv \exp\left[\frac{i\pi M(\mathbf{q}_0,\mathbf{q}_t)}{2}\right]|d\mathbf{q}_t|^{1/2}, \tag{28}$$

with $d\mathbf{q}_t^{1/2*}$ being the complex conjugate to $d\mathbf{q}_t^{1/2}$. Then, Eq. (24) is rewritten in a symmetric form as

$$F(\mathbf{q}_t,t)d\mathbf{q}_t^{1/2} = F(\mathbf{q}_0,0)d\mathbf{q}_0^{1/2}, \tag{29}$$

which expresses the "conservation rule" up to the phase [64].

IV. SEMICLASSICS IN THE LAGRANGE PICTURE WITHOUT THE STABILITY MATRIX

We resume the study of ADF semiclassical equation in the Lagrange picture, that is, Eq. (13). The largest difference of this equation from Eq. (21) is that only the momentum gradient term, $-\frac{1}{2}(\nabla\cdot\mathbf{p})F$, should be explicitly evaluated without regard to the term of $\mathbf{p}\cdot\nabla F$. This brings about great simplicity and theoretical advantage as shown in the following.

A. Analysis of the momentum gradient leading to the deviation determinant

Define the Hessian matrix of the action function S as

$$\mathbf{S}'' = \mathsf{M}\left[\frac{\partial^2 S}{\partial q_I \partial q_J}\right], \tag{30}$$

where $\{q_I | I = 1,\ldots,N\}$ is a set of independent variables in configuration space around a path point under study. The momentum gradient is a trace of this Hessian

$$\sum_J \frac{\partial p_J}{\partial q_J} = \mathrm{Tr}\mathbf{S}'', \tag{31}$$

and therefore it is invariant with respect to the rotation of the coordinate system.

Let us integrate the momentum gradient of the Jth component for a short-time interval $[t,t+\Delta t]$ along a phase space flow $\{q_J^0(t),p_J^0(t)|J=1,\ldots,N\}$. In the Lagrange picture, this integral is approximated as

$$\begin{aligned}\int_t^{t+\Delta t} dt\frac{\partial p_J}{\partial q_J} &\simeq \int_t^{t+\Delta t} dt\frac{p_J - p_J^0}{q_J - q_J^0}\\ &= \int dt\frac{1}{q_J - q_J^0}\frac{d}{dt}\left(q_J - q_J^0\right) \quad (m_J = 1)\\ &= \ln\frac{q_J(t+\Delta t) - q_J^0(t+\Delta t)}{q_J(t) - q_J^0(t)}.\end{aligned} \tag{32}$$

We should note that the value of the relative momentum $p_J - p_J^0$ should be taken in the direction of the relative displacement $q_J - q_J^0$, and (q_J,p_J) must be close to (q_J^0,p_J^0). Then, we continue as

$$\begin{aligned}&\exp\left[\int_t^{t+\Delta t} dt\sum_J \frac{\partial^2 S}{\partial q_J \partial q_J}\right]\\ &= \prod_J\left(\frac{q_J(t+\Delta t) - q_J^0(t+\Delta t)}{q_J(t) - q_J^0(t)}\right) \qquad (33)\\ &= \frac{\det\sigma(t+\Delta t)}{\det\sigma(t)}, \qquad (34)\end{aligned}$$

where the deviation determinant $\sigma(t)$ is defined as

$$\begin{aligned}\sigma(t) &= \prod_J \wedge\left[q_J(t) - q_J^0(t)\right]\mathbf{e}_J\\ &= \prod_J \wedge \sigma_J(t)\mathbf{e}_J,\end{aligned} \tag{35}$$

with $\mathbf{e}_J$ being the unit vector in the Jth direction and $\sigma_J(t) \equiv q_J(t) - q_J^0(t)$.

B. Momentum gradient approximated with nearby classical paths

The above straightforward evaluation of the momentum gradient can be performed only when the action function S is available as a function of independent variables. However, this is not the case in practice. Therefore, we need to extract the essential information of $\sigma(t)$ from the actual dynamics of classical trajectories.

1. Preliminary transformation

Let

$$[\mathbf{q}^0(t),\mathbf{p}^0(t)] \tag{36}$$

be a reference path for which the momentum gradient is considered. To represent the deviation determinant explicitly with classical trajectories, we consider N paths running nearby the reference path

$$[\mathbf{q}^i(t),\mathbf{p}^i(t)], \quad i = 1,\ldots,N \tag{37}$$

which are supposed to satisfy appropriate initial conditions and running on the prespecified action plane S. First, define deviation vectors

$$\Delta\mathbf{q}^i(t) = \mathbf{q}^i(t) - \mathbf{q}^0(t). \tag{38}$$

Orthogonalize these deviation vectors with, for instance, the Gram-Schmidt method and attain a transformation matrix C such that

$$\Delta\mathbf{Q}^K(t) = \sum_i C_{Ki}\Delta\mathbf{q}^i(t) = \sum_i C_{Ki}[\mathbf{q}^i(t) - \mathbf{q}^0(t)] \tag{39}$$

and

$$\Delta\mathbf{Q}^K(t)\cdot\Delta\mathbf{Q}^L(t) = 0 \quad \text{if} \quad K \neq L. \tag{40}$$

The transformation matrix C is parametrically dependent on time, but not a dynamical quantity. It is regarded as a constant at each time of this mathematical operation. Let us define a unit vector $\mathbf{e}_K$ in the direction of the $\Delta\mathbf{Q}^K(t)$ for each K. Then, we extract the scalar part from $\Delta\mathbf{Q}^K(t)$ such that

$$\Delta\mathbf{Q}^K(t) = \Delta Q^K(t)\mathbf{e}_K. \tag{41}$$

Next, with this transformation matrix, we create associated momentum vectors as

$$\Delta \mathbf{P}^K(t) = \sum_i C_{Ki} \Delta \mathbf{p}^i(t) = \sum_i C_{Ki} \frac{d}{dt}[\mathbf{q}^i(t) - \mathbf{q}^0(t)]. \quad (42)$$

However, $\Delta \mathbf{P}^K(t)$ is not parallel to $\Delta \mathbf{Q}^K(t)$ in general. Hence, we extract the parallel component by defining

$$\Delta P_\parallel^K(t) = \Delta \mathbf{P}^K(t) \cdot \mathbf{e}_K. \quad (43)$$

With these quantities, we can evaluate the momentum gradient approximately as

$$\frac{\partial p_k}{\partial q_k} \simeq \frac{\Delta P_\parallel^K(t)}{\Delta Q^K(t)}. \quad (44)$$

We then formally borrow the formula of Eq. (32):

$$\int_t^{t+\Delta t} dt \frac{\Delta P_\parallel^K(t)}{\Delta Q^K(t)} = \int dt \frac{1}{\Delta Q^K(t)} \frac{d}{dt}[\Delta Q^K(t)] = \ln \frac{\Delta Q^K(t+\Delta t)}{\Delta Q^K(t)}, \quad (45)$$

where we have used again the mass-scaled coordinates. Therefore, we have

$$\exp\left[-\frac{1}{2}\int_t^{t+\Delta t} dt \sum_k \frac{\partial p_k}{\partial q_k}\right] = \left[\prod_{k=1}^N \frac{\Delta Q^K(t)}{\Delta Q^K(t+\Delta t)}\right]^{1/2}. \quad (46)$$

Thus, $\sigma(t)$ is approximately represented as

$$\sigma(t) = \prod_{K=1}^N \Delta Q^K(t) = \prod_{k=1}^N \wedge [\Delta Q^K(t) \mathbf{e}_K],$$

which is an orientable volume of the N-dimensional cuboid-like manifold formed around $\mathbf{q}^0(t)$. It is obvious from the property of the wedge product that $\sigma(t)$ can be rewritten in terms of the original nearby trajectories before the orthogonalization such that

$$\sigma(t) = \prod_{i=1}^N \wedge [\mathbf{q}^i(t) - \mathbf{q}^0(t)]. \quad (47)$$

We call $\mathbf{q}^i(t) - \mathbf{q}^0(t)$ the ith deviation vector.

2. *Deviation matrix*

Since $\sigma(t)$ is invariant with respect to the choice of coordinates in configuration space, one may write it as follows. Let

$$\mathbf{q}^i(t) = \left[x_1^i(t), x_2^i(t), \ldots, x_N^i(t)\right] \quad (48)$$

be a configuration-space point of a nearby path of a reference trajectory

$$\mathbf{q}^0(t) = \left[x_1^0(t), x_2^0(t), \ldots, x_N^0(t)\right]. \quad (49)$$

Consider small deviation vectors measured from the reference trajectory at $t = 0$, which are denoted as

$$\mathbf{q}^i(0) - \mathbf{q}^0(0) = \left[x_1^0(0), x_2^0(0), \ldots, x_i^0(0) + \Delta x_i(0), \ldots, x_N^0(0)\right]$$

with $i = 1, 2, \ldots, N$. The deviations are all supposed to be very small, and the volume of a box made of these vectors is simply

$$\sigma(0) = \prod_{i=1}^N \Delta x_i(0).$$

These deviation vectors are evolved in time along the classical flows (with a given initial condition) such that

$$\mathbf{q}^i(t) - \mathbf{q}^0(t) = \left[x_1^0(t) + \Delta x_1^{(i)}(t), \ldots, x_i^0(t) + \Delta x_i^{(i)}(t), \ldots, x_N^0(t) + \Delta x_N^{(i)}(t)\right].$$

We can then express $\sigma(t)$ in terms of a determinant

$$\sigma(t) = \prod_{i=1}^N \wedge [\mathbf{q}^i(t) - \mathbf{q}^0(t)] = \begin{vmatrix} \Delta x_1^{(1)}(t) & \ldots & \Delta x_1^{(j)}(t) & \ldots & \Delta x_1^{(N)}(t) \\ \vdots & & \vdots & & \vdots \\ \Delta x_i^{(1)}(t) & \ldots & \Delta x_i^{(j)}(t) & \ldots & \Delta x_i^{(N)}(t) \\ \vdots & & \vdots & & \vdots \\ \Delta x_N^{(1)}(t) & \ldots & \Delta x_N^{(j)}(t) & \ldots & \Delta x_N^{(N)}(t) \end{vmatrix}. \quad (50)$$

$\sigma(t)$ is thus called deviation determinant, the matrix of which is accordingly called deviation matrix.

Incidentally, the minor determinant of the stability matrix $[\partial \mathbf{q}_t / \partial \mathbf{q}_0]$ is similarly represented as

$$[\partial \mathbf{q}_t / \partial \mathbf{q}_0] = \lim_{\substack{\Delta x_1(0) \to 0 \\ \vdots \\ \Delta x_N(0) \to 0}} \begin{pmatrix} \Delta x_1^{(1)}(t)/\Delta x_1(0) & \ldots & \Delta x_1^{(j)}(t)/\Delta x_j(0) & \ldots & \Delta x_1^{(N)}(t)/\Delta x_N(0) \\ \vdots & & \vdots & & \vdots \\ \Delta x_i^{(1)}(t)/\Delta x_1(0) & \ldots & \Delta x_i^{(j)}(t)/\Delta x_j(0) & \ldots & \Delta x_i^{(N)}(t)/\Delta x_N(0) \\ \vdots & & \vdots & & \vdots \\ \Delta x_N^{(1)}(t)/\Delta x_1(0) & \ldots & \Delta x_N^{(j)}(t)/\Delta x_j(0) & \ldots & \Delta x_N^{(N)}(t)/\Delta x_N(0) \end{pmatrix}. \quad (51)$$

On the other, the momentum gradient is simply given as

$$\exp\left[-\frac{1}{2}\int_0^t dt\sum_k\frac{\partial p_k}{\partial q_k}\right]=\frac{\sigma(t)^{-1/2}}{\sigma(0)^{-1/2}}. \tag{52}$$

It therefore follows that

$$\sum_k\frac{\partial p_k}{\partial q_k}=\frac{\dot\sigma(t)}{\sigma(t)}=\frac{d}{dt}\ln\sigma(t), \tag{53}$$

which is a useful identity that holds when all the deviation vectors collectively approach zero.

Thus, ADF propagated by the momentum gradient alone is given as

$$\begin{aligned}&F(\mathbf{q}-\mathbf{q}(t+\Delta t),t+\Delta t)|_{\mathbf{q}=\mathbf{q}(t+\Delta t)}\\&=\exp\left[-\frac{1}{2}\int_t^{t+\Delta t}dt\sum_k\frac{\partial p_k}{\partial q_k}\right]F(\mathbf{q}-\mathbf{q}(t),t)\\&=\left(\frac{\sigma(t)}{\sigma(t+\Delta t)}\right)^{1/2}F(\mathbf{q}-\mathbf{q}(t),t)|_{\mathbf{q}=\mathbf{q}(t)}.\end{aligned} \tag{54}$$

This relation is rewritten in a form of "norm conservation up to phase" such that

$$\begin{aligned}&\sigma(t+\Delta t)^{1/2}F(\mathbf{q}-\mathbf{q}(t+\Delta t),t+\Delta t)|_{\mathbf{q}=\mathbf{q}(t+\Delta t)}\\&=\sigma(t)^{1/2}F(\mathbf{q}-\mathbf{q}(t),t)|_{\mathbf{q}=\mathbf{q}(t)},\end{aligned} \tag{55}$$

which should be compared with Eq. (29).

3. *Maslov phase arising from the deviation determinant*

A divergence is expected at a point where $\sigma(t)=0$ and a new phase arises in Eq. (55) when the deviation determinant passes across zero and the sign changes as $\sigma(t+\Delta t)\sigma(t)<0$. It is obvious in comparing Eqs. (51) and (52) that the points of the change of the Maslov index are the same. Therefore, the Maslov index in the Euler and Lagrange pictures is exactly the same as they should be (recall that both the Euler and Lagrange pictures should give the same results as they start from exactly the same differential equation). Indeed, we have made use of the deviation determinant to calculate the Maslov index before in a semiclassical ADF in the Euler picture [74]. Incidentally, a comparison between Eqs. (50) and (51) gives an idea that the stability matrix can be approximated in terms of nearby orbits as in the calculation of the momentum gradient. In fact, such a method has been suggested [75] and proposed before [43].

C. Rescaling the deviation determinant of $\sigma(t)$

Advantages of the deviation matrix over the stability matrix are as follows: (i) There is no need to integrate $2N\times 2N$ ordinary differential equations along each reference path. (ii) No Hessian matrix of the potential function with respect to the coordinates is required, direct computation of which are time consuming and tedious for *ab initio* PES (see [32] to improve the related difficulty). On the other hand, we need N of nearby paths to calculate a deviation matrix for a single path, so that it scales to N. However, it should be noted that those nearby orbits are also surrounded by other nearby orbits, and hence a nearby orbit can be regarded as a reference path that is surrounded by other nearby paths. Therefore, computational time should depend on how efficiently the relevant computational algorithm is designed.

On the other hand, nearby orbits with which to calculate the deviation matrix can deviate from a reference path as time passes. The situation is expected to be worse as chaoticity of underlying dynamics becomes harder. (Computation of the stability matrix also faces severe difficulty.) Such a property of the deviation determinant can become a serious disadvantage. In such a case, the difference approximation in Eq. (44) loses the mathematical sense, and therefore we should rescale the deviation vector $[\mathbf{q}^i(t)-\mathbf{q}^0(t),\mathbf{p}^i(t)-\mathbf{p}^0(t)]$ in such a manner that the momentum gradient is to be conserved. This procedure can be achieved as follows: Consider an approximation to the momentum gradient before neighboring paths deviate much in such a way that a factor A is multiplied without changing the approximate expression of the momentum gradient as

$$\frac{|\mathbf{p}^i(t)-\mathbf{p}^0(t)|}{|\mathbf{q}^i(t)-\mathbf{q}^0(t)|}=\frac{|\mathbf{p}^i(t)-\mathbf{p}^0(t)|\times A}{|\mathbf{q}^i(t)-\mathbf{q}^0(t)|\times A}. \tag{56}$$

Then, a new phase-space point $[\mathbf{q}^{i,\mathrm{new}}(t),\mathbf{p}^{i,\mathrm{new}}(t)]$ is attained, which is closer to the reference path, as

$$\mathbf{q}^{i,\mathrm{new}}(t)=\mathbf{q}^0(t)+[\mathbf{q}^i(t)-\mathbf{q}^0(t)]\times A \tag{57}$$

and

$$\mathbf{p}^{i,\mathrm{new}}(t)=\mathbf{p}^0(t)+[\mathbf{p}^i(t)-\mathbf{p}^0(t)]\times A. \tag{58}$$

This procedure is somewhat analogous to the method figured out by Benettin *et al.* [76] for the calculation of the Liapunov exponents to measure the stability of classical trajectories.

Recalling Eq. (54), we notice that the deviation vectors around a reference trajectory in a time interval $[t,t+\Delta t]$ can be different from those of $[t+\Delta t,t+2\Delta t]$ as long as we resort to the Trotter decomposition, that is,

$$\begin{aligned}&F(\mathbf{q}-\mathbf{q}(t+2\Delta t),t+2\Delta t)^{mg}\\&=\exp\left[\int_{t+\Delta t}^{t+2\Delta t}\left(-\frac{1}{2}\nabla\cdot\mathbf{p}\right)\right]\\&\quad\times\exp\left[\int_t^{t+\Delta t}\left(-\frac{1}{2}\nabla\cdot\mathbf{p}\right)\right]F(\mathbf{q}-\mathbf{q}(t),t).\end{aligned} \tag{59}$$

Thus, we have

$$\begin{aligned}&F(\mathbf{q}-\mathbf{q}(t+2\Delta t),t+2\Delta t)^{mg}\\&=\frac{\sigma(t+\Delta t)^{-1/2}}{\sigma(t+2\Delta t)^{-1/2}}\frac{\sigma(t)^{-1/2}}{\sigma(t+\Delta t)^{-1/2}}F(\mathbf{q}-\mathbf{q}(t),t)\end{aligned} \tag{60}$$

and $\sigma(t+\Delta t)$ is canceled. However, the deviation vectors to be used in $[t,t+\Delta t]$ and $[t+\Delta t,t+2\Delta t]$ may be different under a certain condition. The rescaling technique developed above is one of them. In this well-defined context, we may write

$$\begin{aligned}&F(\mathbf{q}-\mathbf{q}(t+2\Delta t),t+2\Delta t)^{mg}\\&=\frac{\sigma^{re}(t+\Delta t)^{-1/2}}{\sigma^{re}(t+2\Delta t)^{-1/2}}\frac{\sigma(t)^{-1/2}}{\sigma(t+\Delta t)^{-1/2}}F(\mathbf{q}-\mathbf{q}(t),t),\end{aligned} \tag{61}$$

where $\sigma^{re}(t+\Delta t)$ and $\sigma^{re}(t+2\Delta t)$ are given in a rescaled vector. Taking the ratio appropriately in each time interval is essential in this calculation.

D. On the initial conditions: Caustics or turning points

In applications of semiclassical mechanics, the choice of initial conditions needs a special care since different choice of initial wave packet leads to divergence at different points. It is a standard practice to choose a coherent-type Gaussian wave function, which is of the form in one-dimensional example as

$$\psi_c(x,0) = \pi^{-1/4} \exp\left[-\frac{1}{2}(x-x_0)^2 + \frac{i}{\hbar}p_0(x-x_0)\right]. \quad (62)$$

We set the exponent to $\frac{1}{2}$. This function is like the minimum uncertainty coherent wave packet, except that the width parameter is fixed. For this initial wave packet, nearby trajectories should be placed close to x_0 with the same initial momentum p_0 as that of the reference path. As is well known, the resultant divergence is found at the so-called caustic points of each reference. Yet, other choices are equally possible. For instance, let us consider the following form:

$$\psi_t(x,0) = \pi^{-1/4} \exp\left[-\frac{1}{2}(x-x_0)^2 + \frac{i}{\hbar}p_0(x-x_0) + \frac{i}{\hbar}\frac{1}{2}\frac{\partial p}{\partial x}\bigg|_0 (x-x_0)^2\right], \quad (63)$$

in which the second-order derivative of the initial action function is assumed to take a nonzero value $[(1/2)\partial p/\partial x|_0 = (1/2)\partial^2 S/\partial x^2|_0]$. Here again, $\hbar$ is absent in the Gaussian width. This initial wave packet brings about divergence in ADF at the so-called turning points.

To see the difference of the above functions, let us visualize the phase-space geometry for them in terms of the Wigner phase-space distribution function, which is defined as [9]

$$W(x,p) = \frac{1}{2\pi\hbar}\int \psi^*(x+r/2)\psi(x-r/2)e^{ipr/\hbar}dr. \quad (64)$$

The functions $\psi_c(x,0)$ and $\psi_t(x,0)$ of Eqs. (62) and (63), respectively, are mapped onto phase space with the forms of

$$W_c(x,p) = 2\exp[-(x-x_0)^2]\exp\left[-\frac{1}{\hbar^2}(p-p_0)^2\right], \quad (65)$$

$$W_t(x,p) = 2\exp[-(x-x_0)^2] \times \exp\left[-\frac{1}{\hbar^2}\left((p-p_0) - \frac{\partial p}{\partial x}\bigg|_0 (x-x_0)\right)^2\right]. \quad (66)$$

In Fig. 1, contour plots are drawn in phase space for the functions of Eqs. (65) and (66) with selected magnitudes of the Planck constant $\hbar$. We simply consider the dynamics of these phase-space distributions for a harmonic oscillator, without loss of generality, for which phase-space trajectories can be always rescaled to concentric circles.

As confirmed in the figure [Figs. 1(a)–1(c) and 1(A)–1(C)], the phase-space distributions become thinner to a straight-line segment as the Planck constant becomes smaller. Furthermore, the straight segment for the initial wave function (62) is parallel to the x axis, while that of Eq. (63) lies tangential to the relevant circle. Note that in Eq. (63) the coefficient $\frac{1}{2}$ multiplied to $\partial p/\partial x$ has naturally vanished in transforming to the Wigner representation.

Then, we track semiclassical time propagation of the distributions in the small limit of $\hbar$. As time passes, the orientations of those line segments change continuously, and they come to two points during one circuit, at which the

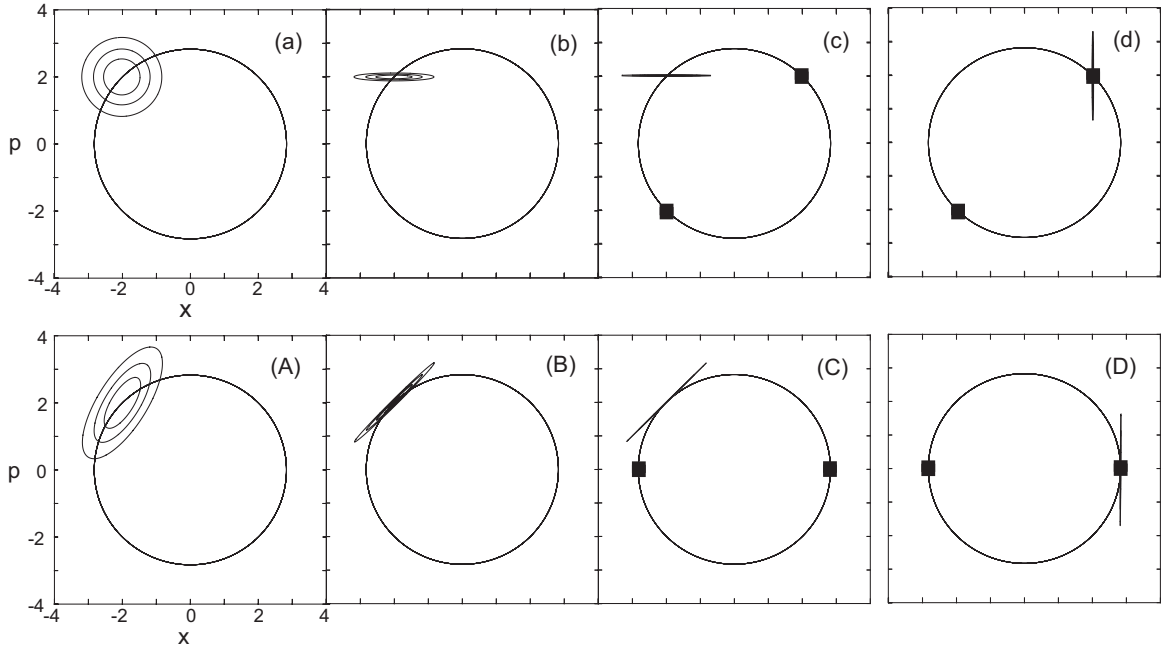

FIG. 1. Contours for the Wigner phase-space representations of the initial wave functions ψ_c (upper panels) and ψ_t (lower panels). Values of the Planck constant $\hbar$ are 1.0 for (a) and (A), 0.1 for (b) and (B), and 0.01 for (c) and (C). Filled squares in panels (c) and (d) are the caustics, while those in (C) and (D) are turning points. In (d) and (D), the line segments are in the singular configurations.

segments become perpendicular to the x axis. It is at these points that the projection of these manifolds becomes singular geometrically or, equivalently, the gradient $\partial p/\partial x$ becomes divergent analytically. The singular points for the initial wave function of Eq. (62) are called caustics [Fig. 1(d)]. On the other hand, we observe the singularity for Eq. (63) at the so-called turning points, at which the kinetic energy is zero [Fig. 1(D)]. Thus, the turning points play a characteristic role not only in stationary-state semiclassical theory, but even in the "time-dependent" semiclassics. Likewise, one may expect divergence in $\partial x/\partial p$ when projecting from phase space onto momentum space.

Finally, it should be confirmed that these singular behaviors are resolved in phase-space quantum mechanics, in which no projection from phase space to configuration space is demanded. Moreover, the smoothed manifolds with a larger Planck constant, as in Figs. 1(a) and 1(A), never face such singularity. Incidentally, the idea of Gaussian wave packet with its phase-space representation not being aligned with x and p axes has been already been proposed by Heller in the contexts of both time-dependent [77] and stationary [78] wave functions.

V. NUMERICAL TESTS

Here in this section, some numerical results are presented to test the accuracy of semiclassical ADF in the Lagrange picture and the validity of rescaling procedure of the deviation vectors. The validity range of the semiclassical ADF is also examined.

A. One- and two-dimensional examples of propagation of wave packets

First of all, one-dimensional Morse oscillator is used to generate a global wave function at a time, the potential of which is

$$V(s) = D_e[1 - e^{-\alpha(s-s_e)}]^2, \tag{67}$$

with the parameters $m = 1.165 \times 10^5$, $D_e = 0.05717$, $s_e = 5.039$, $\alpha = 0.9830$ in atomic units [79,80]. The values of wave function given by ADF with the momentum gradient are directly compared with those of the fully quantum (FQ) counterpart. The latter is obtained with numerical integration of the Schrödinger equation with the symplectic integrator fast Fourier transform (FFT) method [81]. A coherent-state wave packet with an initial phase-space point $p_0 = 0$, $q_0 = 4.535$, $E_0 = 0.02342$ (in a.u.), and $\hbar = 1.0$ is adopted. The initial condition is chosen to be the coherent-type Gaussian function of Eq. (62). The values of ADF at each (q,t) are computed accordingly, that is, trajectories with the same p_0 are prepared at $t = 0$ on the equally spaced grid points, each of which is classically propagated carrying a delta-function-like $F(q - q(t),t)$ on it. The whole ADF wave function is constructed by taking a superposition of contributions in each bin at any time. Figure 2 shows a snapshot after ≈3.5 oscillations. The number of trajectories used is as many as 10 000 for this pointwise comparison.

As seen in Fig. 2, the wave function is oscillatory enough and serves as a stringent test. The ADF undergoes divergence at caustic points, as is expected from the above mathematical

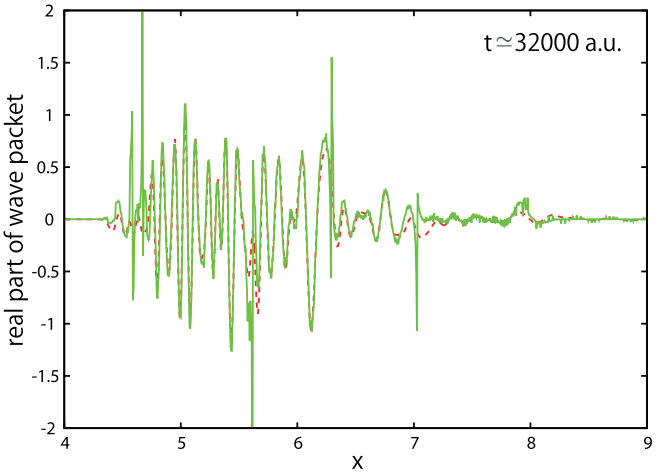

FIG. 2. (Color) Comparison of the real part of wave packets after ≈3.5 oscillations as a function of the coordinate x (in atomic units). (Red, dashed curve) Fully quantum wave packet. (Green, solid curve) Semiclassical ADF wave packet obtained with only the momentum gradient operation. Both are in good agreement except for some points where sampled trajectories happen to encounter singular points.

consideration. Note that it shows nevertheless quite a good performance except for these specific points. It is seen that ADF wave packet reproduces the oscillatory behavior of FQ wave packet on this potential.

Next, as a two-dimensional test, the following modified Hénon-Heiles Hamiltonian is used:

$$H(x,y,p_x,p_y) = \frac{p_x^2}{2m} + \frac{p_y^2}{2m} + \frac{x^2+y^2}{2} + x^2(0.6y^2 + y) + \frac{1}{3}y^3(0.2y - 1) + 0.1x. \tag{68}$$

In this test, we examine a wave-packet component carried on a single classical trajectory. Suppose we have a two-dimensional coherent-state-like Gaussian wave packet at $t = 0$:

$$F(q - q(0),0) = \left(\frac{1}{\pi\hbar}\right)^{1/2} \times \exp\left[-(\mathbf{q} - \mathbf{q}_0)\cdot\mathbf{M}\cdot(\mathbf{q} - \mathbf{q}_0)^T + \frac{i}{\hbar}\mathbf{p}_0\cdot(\mathbf{q} - \mathbf{q}_0)\right], \tag{69}$$

$$\mathbf{M} = \begin{pmatrix} \frac{1}{2\hbar\times w} & 0 \\ 0 & \frac{1}{2\hbar\times w} \end{pmatrix}, \tag{70}$$

where $\mathbf{q} - \mathbf{q}_0 = (x - x_0, y - y_0)^T$ and $\mathbf{p}_0 = (p_{x_0}, p_{y_0})$. In the FQ dynamics, this wave packet is propagated based on the time-dependent Schrödinger equation. On the other hand, a value of ADF at each space-time point is supposed to be carried by ADF along a classical trajectory, and therefore in this test $F(\mathbf{q} - \mathbf{q}(t),t)$ initially located at $(\mathbf{q}_0,\mathbf{p}_0)$ is tracked. Since we would like to follow the wave-packet component in the semiclassical limit, the Planck constant is set to $\hbar = 0.001$. Note that the Gaussian width is tuned with an adjustment parameter w, which is set to be $w = 5$ here.

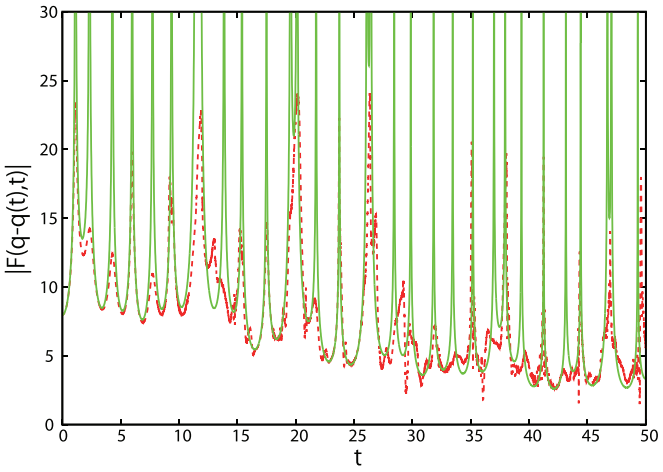

FIG. 3. (Color) Semiclassical ADF wave-packet height $|F(\mathbf{q}-\mathbf{q}(t),t)|$ calculated along the central classical trajectory with $(\mathbf{q}_0,\mathbf{p}_0)$ (green solid curve) is compared with the FQ counterpart on the same trajectory (red dashed curve). Except for the divergent behaviors in the neighborhood of classical singular points (caustics), agreement between the two is very good.

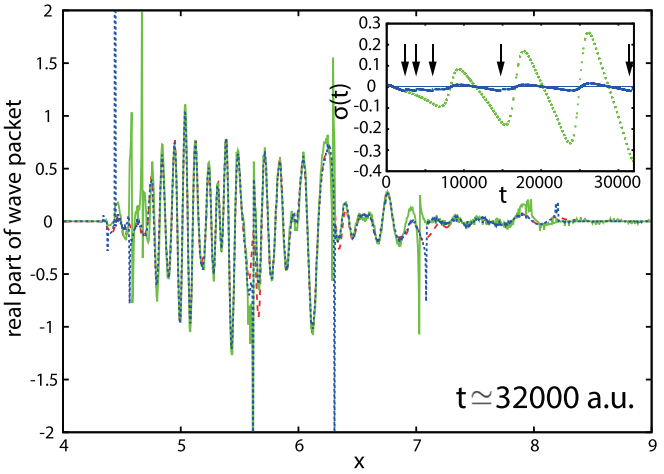

FIG. 4. (Color) Effect of the rescaling on the spatial distributions of wave functions after about 3.5 oscillations, with the dynamics being the same as that of Fig. 2. (Red, dashed curve) Real part of fully quantum wave packet. (Green, solid curve) Semiclassical ADF wave packet without rescaling. (Blue, dotted curve) Semiclassical ADF wave packet with rescaling. The difference between the wave-packet behaviors with and without the rescaling happens not to be large in this example, although the former has improved the latter. In the inset are shown the time evolutions of $\sigma(t)$. Without rescaling, $\sigma(t)$ evolves with its absolute value getting larger and larger, while passing through zeros at the caustics (green dashed curve). Rescaling has been performed at times indicated by arrows when $\sigma(t)$ gets larger than $\zeta = 2\times\sigma(0)$ (blue solid curve).

Although $F(\mathbf{q}-\mathbf{q}(t),t)$ has information about both height and phase, only the wave-packet height is compared because the small value of $\hbar$ makes the real and imaginary parts too oscillatory to compare visually. The energy chosen in Fig. 3 is $E \simeq 0.135$. This figure shows that divergent behavior begins to be noticeable in time regions when the classical trajectory approaches caustics. However, again it is clear that except for those points, the height of the wave packet is very well reproduced by ADF.

B. Validity of the rescaling of the nearby trajectories

Next, we numerically examine whether the rescaling procedure for the deviation vector [Eq. (56)] is indeed valid. We have applied the rescaling procedure several times to the dynamics shown in Fig. 2, the resultant wave function being displayed in Fig. 4. In this figure, semiclassical ADF with rescaling (blue curve), semiclassical ADF without rescaling (green curve), and the full quantum counterpart are superposed. In the inset of the figure, $\sigma(t)$ (actually the length of the deviation vector) without rescaling is drawn in a green curve. $\sigma(t)$ is rescaled and nearby trajectories are correspondingly renewed to be closer to the reference when $\sigma(t)$ exceeds a predetermined threshold value ζ. In Fig. 4, the threshold value is set to $\zeta = 2\times\sigma(0)$. It is seen that $\sigma(t)$ becomes larger as time passes, which eventually makes ADF very small, except for the singular points. In this inset, the occasions at which we applied the rescaling are marked with arrows. Due to the rescaling, $\sigma(t)$ is kept as small as in the initial level. In spite of the fact that $\sigma(t)$ is thus largely modulated, the resultant semiclassical wave functions (blue and green curves in Fig. 4) happen to be close to each other in this example. This suggests that the amplitude of the semiclassical ADF may be rather insensitive to the variation of $\sigma(t)$, provided that it remains in a tolerable range. This also implies that ADF should not be very sensitive to the choice of $\sigma(0)$, the initial deviation determinant. (More careful inspection over the figure suggests, however, that far longer continuation without rescaling should result in a bad wave function.) We have also successfully tested the method in two-dimensional cases. Thus, the rescaling procedure should be a powerful tool for the ADF wave-packet dynamics even in chaotic systems, in which nearby orbits quickly leave from their reference path. This aspect will be reported elsewhere.

C. Feasibility in many-dimensional semiclassical calculations

Finally, a result of 100-dimensional calculation is shown in Fig. 5, just to show that it is indeed tractable. A Hamiltonian in this test is

$$H = \sum_j^N \frac{p_j^2}{2m} + \sum_j^N \frac{\omega_j}{2}(q_j - R_{0j})^2 - \sum_j^{N-1} D_j(q_{j+1}-q_j)\exp[-\zeta_j(q_{j+1}-q_j)], \qquad (71)$$

where $N = 100$, $m = 1$, $R_{0j} = 2.0\times j$, and $\omega_j = \omega_0 \times (1.013)^j$ with $\omega_0 = 1.0$ ($\omega_{100} \simeq 3.6387$). Couplings are considered only between the neighboring oscillators. $D_j = 1.0$ and $\zeta_j = 0.2$ are the same for all the couplings. The purpose of this test is primarily to show how tractably the semiclassical ADF works for higher-dimensional systems. We follow the ADF in the same way as in the two-dimensional case. That is, the height is tracked along a classical trajectory with the initial condition $(\mathbf{q}_0,\mathbf{p}_0)$, which is randomly picked under a physically appropriate condition. In this system where the individual oscillators have similar frequencies, all the trajectories begin

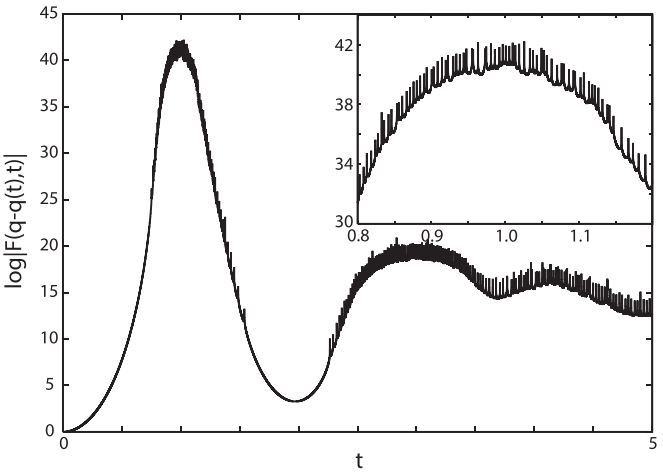

FIG. 5. Semiclassical ADF height $[\log_{10}|F(\mathbf{q}-\mathbf{q}(t),t)|]$ is plotted. The inset is a closeup around the first caustic point encountered. Spikes indicate that $F(\mathbf{q}-\mathbf{q}(t),t)$ is divergent, although all the peak heights are finite due to a discrete time step (Δt has been set to 10^{-5}). Note that in this test the initial wave-packet height is set to unity.

to collectively approach their own caustics, which are close to one another, and hence $\sigma(t)$ soon falls to a very small value resulting in a very rapid increase of the height up to $t = 1.0$. Note that not $|F(\mathbf{q}-\mathbf{q}(t),t)|$ but $\log_{10}|F(\mathbf{q}-\mathbf{q}(t),t)|$ is shown in the figure. In the inset, a closeup of that region is shown, which displays many spikes on top of the globally mountainlike feature. Although all these spikes happen to be of finite height in this graph, each is in fact associated with divergence. This is because our chosen time interval (actually $\Delta t = 10^{-5}$) did not make the exact timing at which $\sigma(t) = 0$ is realized.

Although the calculation shown in Fig. 5 is performed for a shorter time than one period of the first vibrational mode, the present example demonstrates that the computation of $\sigma(t)$ itself is rather easy. We carry over this system to the companion paper [45] to highlight that such gigantic values of the semiclassical ADF, actually full of singularities, are indeed suppressed and smoothed by quantum diffusion.

VI. CONCLUDING REMARKS

We have studied the properties of the action decomposed function towards many-dimensional applications to quantum dynamics of heavy particles as in chemical reactions. The equation of motion for the complex-valued amplitude of ADF represents the coupling between the internal diffusive motion and dynamics of the group velocity in a hierarchical manner ascending from classical to purely quantum mechanics via semiclassical dynamics. It therefore suggests a practical use of mixed quantum-semiclassical-classical representation.

As a first step, we developed a semiclassical approximation in the Lagrange picture. Changing from the Euler to Lagrange picture, we have made a semiclassical formalism without use of the stability matrix. This reformulation has been actually made possible by estimating the semiclassical amplitude with momentum gradient $-\frac{1}{2}(\nabla\cdot\mathbf{p})F(\mathbf{q},t)$ alone. Practically, the height and associated phase of the amplitude factor are represented in terms of the deviation matrix and deviation vectors. In terms of these quantities, a route for incorporating quantum effects in many-dimensional applications has become possible without resorting to the integration of the stability matrix and the Hessian matrix of a potential function [45]. Another advantage of the deviation vectors is that they can be rescaled keeping the magnitude of the momentum gradient invariant, when nearby paths begin to deviate from a reference path.

Numerical tests have shown that semiclassical ADF at each configuration-space point and time along a classical path excellently reproduces the exact wave functions. However, semiclassical ADF is not free of the semiclassical singularity, in other words, the wave function diverges at points where the momentum gradient diverges. As is well known, this divergence takes place at points where classical paths have a focal point in configuration space. The similar situation can happen in momentum space too, and therefore, this singularity problem originates from a mathematical projection from a larger space (phase space of $2N$ dimensions) to a smaller one (an N-dimensional space like configuration space). Therefore, it is in the process of smoothing the singularities that one of the very essential characteristics of quantum mechanics is hidden.

Our next goal is therefore to reveal how quantum mechanics smooths the singularity of semiclassical ADF. Nevertheless, we here conclude this paper up to this stage since this is a branching point in that there can exist several ways to cope with quantum smoothing. We will propose an approach as such in the next paper [45], using the deviation matrix rather than the stability matrix, and show the mathematical mechanism of how quantum mechanics can remove the semiclassical singularity.

ACKNOWLEDGMENTS

We thank Professor R. Wyatt for valuable discussions in the early stage of this work. The appendix is a product after discussion with Dr. T. Yonehara. We also thank M. Konishi for useful discussions. This work was supported in part by a Grant-in-Aid for Scientific Research from the Ministry of Education and Science in Japan.

APPENDIX: ADF IN CLASSICAL ELECTROMAGNETIC VECTOR FIELDS

The ADF formalism can be applied to particle dynamics under a (classical) vector potential (see also Ref. [47]). We formulate it to see below how it looks. We begin with the following nonrelativistic Schrödinger equation:

$$i\hbar\frac{\partial}{\partial t}\Psi(\mathbf{q},t) = \left[\frac{1}{2}\sum_k \frac{1}{m_k}\left(\hat{p}_k - \frac{Z_k e}{c}A_k(\mathbf{q})\right)^2 + V(\mathbf{q})\right] \times\Psi(\mathbf{q},t), \tag{A1}$$

where $\hat{p}_k$ is the quantum momentum operator

$$\hat{p}_k = \frac{\hbar}{i}\frac{\partial}{\partial q_k} \tag{A2}$$

and should be distinguished from its classical counterpart p_k. Here again, we resort to the mass-weighted coordinates, rescaling all the masses to

$$m_k = 1. \tag{A3}$$

The momentum of a particle is correlated with its momentum in such a way that

$$v_k = \frac{1}{m_k}\left(p_k - \frac{Z_k e}{c}A_k(\mathbf{q})\right). \tag{A4}$$

The classical counterpart of this dynamics is represented in the following Hamilton-Jacobi equation:

$$\frac{\partial}{\partial t}S(\mathbf{q},t) + \frac{1}{2}\sum_k\left(\frac{1}{m_k}\frac{\partial S(\mathbf{q},t)}{\partial q_k} - \frac{Z_k e}{c}A_k(\mathbf{q})\right)^2 + V(\mathbf{q}) = 0, \tag{A5}$$

where the momentum is generated through the action integral as

$$p_k = \frac{\partial S(\mathbf{q},t)}{\partial q_k}. \tag{A6}$$

It is convenient to summarize the classical relations as

$$\left(\frac{\partial S(\mathbf{q},t)}{\partial q_k} - \frac{Z_k e}{c}A_k(\mathbf{q})\right) = v_k = p_k - \frac{Z_k e}{c}A_k(\mathbf{q}).$$

As before, we set a total wave function in the form

$$\Psi(\mathbf{q},t) = \exp\left(\frac{i}{\hbar}S(\mathbf{q},t)\right)F(\mathbf{q},t). \tag{A7}$$

The left-hand side of the Schrödinger equation is

$$i\hbar\frac{\partial\Psi(\mathbf{q},t)}{\partial t} = \exp\left(\frac{i}{\hbar}S(\mathbf{q},t)\right) \times\left(-\frac{\partial S(\mathbf{q},t)}{\partial t}F(\mathbf{q},t) + i\hbar\frac{\partial F(\mathbf{q},t)}{\partial t}\right). \tag{A8}$$

Next, we evaluate the right-hand side. Since the kinetic energy parts are the origin of confusion, we should treat them with some care. First,

$$\left(\hat{p}_k - \frac{Z_k e}{c}A_k(\mathbf{q})\right)\exp\left(\frac{i}{\hbar}S(\mathbf{q},t)\right) = \exp\left(\frac{i}{\hbar}S(\mathbf{q},t)\right)\left(p_k - \frac{Z_k e}{c}A_k(\mathbf{q})\right) \tag{A9}$$

and

$$\frac{1}{2}\left(\hat{p}_k - \frac{Z_k e}{c}A_k(\mathbf{q})\right)^2\exp\left(\frac{i}{\hbar}S(\mathbf{q},t)\right) = \frac{1}{2}\exp\left(\frac{i}{\hbar}S(\mathbf{q},t)\right)\left[\left(p_k - \frac{Z_k e}{c}A_k(\mathbf{q})\right)^2 + \hat{p}_k\left(p_k - \frac{Z_k e}{c}A_k(\mathbf{q})\right)\right]. \tag{A10}$$

Then, the following straightforward formulation goes as

$$\begin{aligned}\left[\frac{1}{2}\sum_k\left(\hat{p}_k - \frac{Z_k e}{c}A_k(\mathbf{q})\right)^2 + V(\mathbf{q})\right]\exp\left(\frac{i}{\hbar}S(\mathbf{q},t)\right)F(\mathbf{q},t) &= \exp\left(\frac{i}{\hbar}S(\mathbf{q},t)\right)\left[\frac{1}{2}\left(p_k - \frac{Z_k e}{c}A_k(\mathbf{q})\right)^2 + \frac{1}{2}\hat{p}_k\left(p_k - \frac{Z_k e}{c}A_k(\mathbf{q})\right)\right] \\ &+ \exp\left(\frac{i}{\hbar}S(\mathbf{q},t)\right)\frac{1}{2}\sum_k\hat{p}_k^2F(\mathbf{q},t) \\ &+ \exp\left(\frac{i}{\hbar}S(\mathbf{q},t)\right)\sum_k\left(p_k - \frac{Z_k e}{c}A_k(\mathbf{q})\right)[\hat{p}_k F(\mathbf{q},t)],\end{aligned} \tag{A11}$$

where we have used the long-wavelength approximation

$$\hat{p}_k A_k(\mathbf{q}) = 0 \tag{A12}$$

and

$$\hat{p}_k A_k(\mathbf{q}) f = A_k(\mathbf{q})\hat{p}_k f \tag{A13}$$

for an arbitrary function f. Combining Eqs. (A8) and (A11),

$$\begin{aligned}-\frac{\partial S(\mathbf{q},t)}{\partial t}F(\mathbf{q},t) + i\hbar\frac{\partial F(\mathbf{q},t)}{\partial t} &= \sum_k\left[\frac{1}{2}\left(p_k - \frac{Z_k e}{c}A_k(\mathbf{q})\right)^2 + \frac{1}{2}\hat{p}_k\left(p_k - \frac{Z_k e}{c}A_k(\mathbf{q})\right)\right] \\ &+ \frac{1}{2}\sum_k\hat{p}_k^2F(\mathbf{q},t) + \sum_k\left(p_k - \frac{Z_k e}{c}A_k(\mathbf{q})\right)[\hat{p}_k F(\mathbf{q},t)].\end{aligned}$$

With the help of the Hamilton-Jacobi equation (A5), we have

$$i\hbar\frac{\partial F(\mathbf{q},t)}{\partial t} = \sum_k\left(\frac{\hbar}{2i}\nabla_k v_k - \frac{\hbar^2}{2}\nabla_k^2 + \frac{\hbar}{i}v_k\nabla_k\right)F(\mathbf{q},t),$$

which is rewritten as

$$\frac{\partial F(\mathbf{q},t)}{\partial t} = \left[-\mathbf{v}\cdot\boldsymbol{\nabla} - \frac{1}{2}\boldsymbol{\nabla}\cdot\mathbf{v} + \frac{i}{2}\hbar\nabla^2\right]F(\mathbf{q},t). \tag{A14}$$

Note that this ADF equation is exactly the same as that for field-free systems.

[1] V. P. Maslov and M. V. Fedoriuk, *Semi-Classical Approximation in Quantum Mechanics* (Reidel, Dordrecht, 1981).
[2] L. S. Schulman, *Techniques and Applications of Path Integration* (Wiley, New York, 1981).
[3] W. H. Miller, Adv. Chem. Phys. **25**, 69 (1974).
[4] M. V. Berry, Proc. Phys. Soc. London **89**, 479 (1966).
[5] J. R. Stine and R. A. Marcus, J. Chem. Phys. **59**, 5145 (1973).
[6] M. S. Child and P. M. Hunt, Mol. Phys. **34**, 261 (1977).
[7] J. N. L. Connor and D. Farrely, J. Chem. Phys. **75**, 2831 (1981).
[8] P. Gaspard, D. Alonso, and I. Burghardt, Adv. Chem. Phys. **90**, 105 (1995).
[9] E. Wigner, Phys. Rev. **40**, 749 (1932).
[10] J. E. Moyal, Proc. Cambridge Philos. Soc. **45**, 99 (1949).
[11] W. H. Miller, J. Chem. Phys. **53**, 3578 (1970).
[12] E. J. Heller, J. Chem. Phys. **94**, 2723 (1991).
[13] G. Campolieti and P. Brumer, Phys. Rev. A **50**, 997 (1994).
[14] E. J. Heller, J. Chem. Phys. **62**, 1544 (1975).
[15] E. J. Heller, J. Chem. Phys. **65**, 1289 (1976); R. C. Brown and E. J. Heller, *ibid.* **75**, 186 (1981).

[16] K. Takatsuka, Phys. Rev. Lett. **61**, 503 (1988); Phys. Rev. A **45**, 4326 (1992).
[17] E. J. Heller, J. Chem. Phys. **75**, 2923 (1981).
[18] M. F. Herman and E. Kluk, Chem. Phys. **91**, 27 (1984).
[19] E. Kluk, M. F. Herman, and H. L. Davis, J. Chem. Phys. **84**, 326 (1986).
[20] K. G. Kay, J. Chem. Phys. **100**, 4377 (1994).
[21] W. H. Miller, J. Phys. Chem. A **105**, 2942 (2001).
[22] A. L. Kaledin and W. H. Miller, J. Chem. Phys. **118**, 7174 (2003).
[23] A. L. Kaledin and W. H. Miller, J. Chem. Phys. **119**, 3078 (2003).
[24] M. Ceotto, S. Atahan, G. F. Tantardini, and A. Aspuru-Guzik, J. Chem. Phys. **130**, 234113 (2009).
[25] S. Zhang and E. Pollak, J. Chem. Phys. **121**, 3384 (2004).
[26] J. Tatchen and E. Pollak, J. Chem. Phys. **130**, 041103 (2009).
[27] H. Wang, X. Sun, and W. H. Miller, J. Chem. Phys. **108**, 9726 (1998).
[28] Y. Zhao and W. H. Miller, J. Chem. Phys. **117**, 9605 (2002).
[29] J. Liu and W. H. Miller, J. Chem. Phys. **127**, 114506 (2007).
[30] G. Tao and W. H. Miller, J. Chem. Phys. **130**, 184108 (2009).
[31] J. Tatchen, E. Pollak, G. Tao, and W. H. Miller, J. Chem. Phys. **134**, 134104 (2011).
[32] M. Ceotto, Y. Zhuang, and W. L. Hase, J. Chem. Phys. **138**, 054116 (2013).
[33] J. Ankerhold, M. Salter, and E. Pollak, J. Chem. Phys. **116**, 5925 (2002).
[34] E. Pollak and J. Shao, J. Phys. Chem. A **107**, 7112 (2003).
[35] S. Zhang and E. Pollak, J. Chem. Phys. **119**, 11058 (2003).
[36] S. Zhang and E. Pollak, Phys. Rev. Lett. **91**, 190201 (2003).
[37] D. H. Zhang and E. Pollak, Phys. Rev. Lett. **93**, 140401 (2004).
[38] K. G. Kay, Annu. Rev. Phys. Chem. **56**, 255 (2005).
[39] K. G. Kay, Chem. Phys. **322**, 3 (2006).
[40] G. Hochman and K. G. Kay, Phys. Rev. A **73**, 064102 (2006).
[41] G. Hochman and K. G. Kay, J. Phys. A **41**, 385303 (2008).
[42] G. Hochman and K. G. Kay, J. Chem. Phys. **130**, 061104 (2009).
[43] S. Garashchuk and J. C. Light, J. Chem. Phys. **113**, 9390 (2000).
[44] P. Pulay, Adv. Chem. Phys. **69**, 241 (1987).
[45] K. Takatsuka and S. Takahashi, following paper, Phys. Rev. A **89**, 012109 (2014).
[46] K. Takatsuka and A. Inoue, Phys. Rev. Lett. **78**, 1404 (1997); A. Inoue-Ushiyama and K. Takatsuka, Phys. Rev. A **59**, 3256 (1999).
[47] T. Yonehara and K. Takatsuka, J. Chem. Phys. **132**, 244102 (2010).
[48] R. E. Wyatt, *Quantum Dynamics with Trajectories* (Springer, New York, 2005).
[49] C. L. Lopreore and R. E. Wyatt, Phys. Rev. Lett. **82**, 5190 (1999).
[50] V. A. Rassolov, S. Garashchuk, and G. C. Schatz, J. Phys. Chem. A **110**, 5530 (2006).
[51] D. Babyuk and R. E. Wyatt, J. Chem. Phys. **124**, 214109 (2006); **125**, 064112 (2006).
[52] Á. S. Sanz, F. Borondo, and S. Miret-Artés, Phys. Rev. B **61**, 7743 (2000).
[53] Á. S. Sanz, F. Borondo, and S. Miret-Artés, J. Phys.: Condens. Matter **14**, 6109 (2002).
[54] Á. S. Sanz, F. Borondo, and S. Miret-Artés, Phys. Rev. B **69**, 115413 (2004).
[55] Á. S. Sanz and S. Miret-Artés, *A Trajectory Description of Quantum Processes. I. Fundamentals* (Springer, Berlin, 2012).
[56] Á. S. Sanz and S. Miret-Artés, *A Trajectory Description of Quantum Processes. II. Applications* (Springer, Berlin, 2013).
[57] Y. Goldfarb, I. Degani, and D. J. Tannor, J. Chem. Phys. **125**, 231103 (2006).
[58] Y. Goldfarb and D. Tannor, J. Chem. Phys. **127**, 161101 (2007).
[59] Y. Goldfarb, J. Schiff, and D. J. Tannor, J. Phys. Chem. A **111**, 10416 (2007).
[60] J. Schiff, Y. Goldfarb, and D. J. Tannor, Phys. Rev. A **83**, 012104 (2011).
[61] C.-C. Chou and R. E. Wyatt, J. Chem. Phys. **132**, 134102 (2010).
[62] D. Bohm, Phys. Rev. **85**, 166 (1952); **85**, 180 (1952).
[63] E. Nelson, Phys. Rev. **150**, 1079 (1966).
[64] K. Takatsuka, Phys. Rev. E **64**, 016224 (2001).
[65] K. Hotta and K. Takatsuka, J. Phys. A **36**, 4785 (2003).
[66] S. Takahashi and K. Takatsuka, Phys. Rev. A **70**, 052103 (2004).
[67] S. Takahashi and K. Takatsuka, J. Chem. Phys. **124**, 144101 (2006).
[68] H. Teramoto and K. Takatsuka, J. Chem. Phys. **125**, 194301 (2006).
[69] K. Hotta and K. Takatsuka, J. Chem. Phys. **122**, 174108 (2005).
[70] T. Yamashita and K. Takatsuka, Prog. Theor. Phys. Suppl. **166**, 56 (2007).
[71] K. Takatsuka, S. Takahashi, K. Y. W. Patrick, and T. Yamashita, J. Chem. Phys. **126**, 021104 (2007).
[72] S. Takahashi and K. Takatsuka, J. Chem. Phys. **127**, 084112 (2007).
[73] K. Takatsuka, in *Let's Face Chaos Through Nonlinear Dynamics*, edited by M. Robnik and V. Romanovski, AIP Conference Proceeding Vol. 1076 (Springer, New York, 2008), pp. 235–244.
[74] S. Takahashi and K. Takatsuka, Phys. Rev. A **69**, 022110 (2004).
[75] E. J. Heller, J. Chem. Phys. **65**, 4979 (1976).
[76] G. Benettin, L. Galgani, and J.-M. Strelcyn, Phys. Rev. A **14**, 2338 (1976).
[77] E. J. Heller, in *Chaos and Quantum Physics*, edited by M.-J. Giannoni, A. Voros, and J. Zinn-Justin, Proceedings of the Les Houches Summer School, Session LII (North-Holland, Amsterdam, 1991), pp. 547–664.
[78] M. J. Davis and E. J. Heller, J. Chem. Phys. **71**, 3383 (1979).
[79] J. Y. Fang and C. C. Martens, J. Chem. Phys. **105**, 9072 (1996).
[80] H. Wang, M. Thoss, K. L. Sorge, R. Gelabert, X. Giménez, and W. H. Miller, J. Chem. Phys. **114**, 2562 (2001).
[81] K. Takahashi and K. Ikeda, J. Chem. Phys. **99**, 8680 (1993).